

PAPER • OPEN ACCESS

Influence and safety control of blasting vibration on existing lining for closely tunnel expansion

To cite this article: W Wang *et al* 2019 *IOP Conf. Ser.: Earth Environ. Sci.* **351** 012043

View the [article online](#) for updates and enhancements.

You may also like

- [Enhanced Photoluminescence of PPV Thin Film Coated on a Nanostructured Substrate by Glancing Angle Deposition](#)
T. Karabacak, C. Wiegand, J. Senkevich et al.
- [On algorithms for calculating arterial pulse pressure variation during major surgery](#)
Shaoxiang Sun, Wouter H Peeters, Rick Bezemer et al.
- [Diversifying temporal responses of magnetoactive elastomers](#)
Kai Tan, Xin Wen, Xun Gong et al.



ECS
The
Electrochemical
Society
Advancing solid state &
electrochemical science & technology

DISCOVER
how sustainability
intersects with
electrochemistry & solid
state science research

Influence and safety control of blasting vibration on existing lining for closely tunnel expansion

W Wang^{1,2,6}, Q Yuan^{1,3}, H Jiang^{1,4}, and P S Chen^{1,5}

¹CCCC Second Harbour Engineering Co., Ltd., Wuhan, 430040, China

²Research and Development Center of Transport Industry of Intelligent Manufacturing Technologies of Transport Infrastructure, Wuhan, 430040, China

³Key Laboratory of Large-span Bridge Construction Technology, Ministry of Communications, Wuhan, 430040, China

⁴CCCC Highway Bridges National Engineering Research Center Co., Ltd., Beijing 100088, China

⁵Shaanxi Provincial Major Laboratory for Highway Bridge & Tunnel, School of Highway, Chang'an University, Xi'an, 710064, China

⁶E-mail: wangw2018@foxmail.com

Abstract. Based on the project of Erzhuangke expansion tunnel, this paper aims to investigate the influence of the blasting vibration caused by the expanded tunnel excavation on the adjacent existing lining, then a reasonable safety control criterion is proposed. The 3D finite element analysis, combined with field test, was employed to analyze peak particle velocity (PPV) and the maximum tensile stress of the existing lining under the closely tunnel blasting. The results demonstrate that the blasting vibration attenuation rate of existing lining is faster within the range of about 1.5B from the blasting source, then gradually tends to be flat, and the two sides are basically symmetrical distribution. However, the PPV and tensile stress of the side wall and arch waist of the existing lining nearest to the blasting source are significantly larger than those of other locations, so it is more likely to be damaged. The numerical simulation results are in good agreement with the field test, which also verifies the accuracy of the field test results and the rationality of the numerical simulation. Moreover, the safety control criterion based on the PPV and maximum tensile stress is established to ensure the operation safety of existing tunnels, and the PPV safety criterion of existing lining is 10.73 cm/s, so that the maximum allowable charge of a single section should be controlled within 41.05 kg.

1. Introduction

With the improvement of blasting technology, blasting disasters often occur, especially the damage caused by blasting vibration to adjacent buildings (structures). According to the control standard of blasting safety regulations, the safety of structure is not necessarily ensured. In many cases, when the PPV reaches the safety control standard, no obvious damage or destroy is found in the structure, while when the PPV does not reach the safety standard, the structure is destroyed [1,2]. During tunnel blasting excavation, blasting vibration of different strengths will inevitably cause macro-damage or cumulative damage to underground structures or adjacent buildings (structures), but it is difficult to assess and judge the damage degree of blasting vibration to structures [3]. Therefore, it has attracted



widespread attention from many scholars at home and abroad. The methods to study the impact and safety control problems of tunnel blasting on existing buildings are mainly divided into three categories: 1) Theoretical analysis method, in which the stress wave theory lays the foundation for studying the influence of blasting load on adjacent structures. Based on the stress wave theory, the critical vibration velocity of lining under different incident angles is obtained by using the complex variable function method [4]. Besides, the vibration velocity criterion model to ensure the safety of tunnel lining is established according to the stress wave theory and the ultimate tensile stress criterion [5]. 2) Field test method, the response of blasting vibration can be well reflected by the field test system. The characteristics and regularities of blasting vibration at middle partition wall and excavation face in closed tunnel are discussed according to field test [6]. And the application effect of short step advance and millisecond blasting control technology inside and outside holes in down-penetrating ramp is verified by field test [7]. 3) Numerical analysis method, which is widely used in engineering because of its simplicity, rapidity and high accuracy. The dynamic characteristics of the existing tunnel lining under the blasting action of the following tunnel are studied, and the blasting safety control standard of the branched tunnel is determined by using 3D numerical simulation software of ANSYS/LS-DYNA. Moreover, the effects of different depths, spacing and excavation step on the existing lining are studied through the numerical calculation model of triangular equivalent blasting load [8,9]

In summary, there are few studies on the impact of blasting on existing tunnel lining structure and safety control standards, because different tunnel projects have their own unique characteristics, and there is no similar engineering basis for reference. Therefore, based on the Erzhuangke expansion tunnel project, this paper aims to study the attenuation law and influence of stress wave in existing lining structure under the blasting load of closed distance extension excavation by combining field test with numerical simulation, and then puts forward a reasonable safety criterion blasting control, which can not only guarantee the safe construction of existing tunnels, but also can provide guidance for blasting engineering design and construction.

2. Description of projects

The expansion tunnel is located in the near of Erzhuangke village, Yan'an City. It runs parallel to the existing Erzhuangke tunnel and crosses the same mountain. The existing tunnel length is 640 m from ZK2+027 to ZK2+667, and the new tunnel length is 630 m from YK2+015 to YK2+645, which belongs to the medium-long tunnel (>500 m). The maximum cover on the tunnel is 145 m, and the surrounding rock is mainly composed of strong - medium weathered sandstone. The new tunnel is a one-way three-lane city main road, and the design speed is 50 km/h. Considering the road belt and safety width, the excavation area is more 130.4 m², with a width B of 16.34 m and height of 10.45 m. The location relationship between the existing tunnel and the new tunnel is shown in Figure 1. The distance between the two measuring lines of tunnel is 25 - 42 m and the clear distance is 21 - 38 m.



Figure 1. Location relationship between new tunnel and existing tunnel.

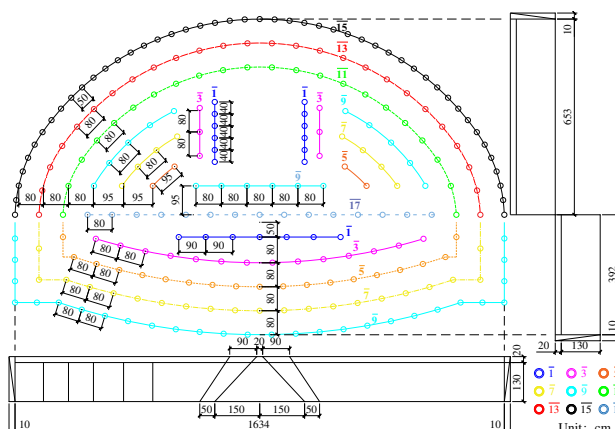


Figure 2. The arrangement of tunnel blasting hole (unit: cm).

Therefore, the difficulty of the project is how to control the blasting influence on the closely existing lining. But the PPV of traffic tunnels is 10 - 20 cm/s referring to “Chinese Blasting Safety Regulations GB 6722-2014” [10], so it cannot be accurately judge the safety state of the structure in actual engineering. The two step method was employed to construct the tunnel, and the cutting holes of upper steps are wedge-shaped, with a vertical depth of 1.50 m, so the specific blasting construction parameters are shown in Table 1. Delay blasting was adopted for tunneling and the blasting design was shown in Figure 2. Each row of blasting holes adopts millisecond delay blasting, and the delay time difference between adjacent detonator sections is 100 ms. The boreholes are divided into 9 groups according to the initiation sequence (different color holes use different detonator groups), which are encoded as $\bar{1}$, $\bar{3}$, $\bar{5}$, $\bar{7}$, $\bar{9}$, $\bar{11}$, $\bar{13}$, $\bar{15}$ and $\bar{17}$ respectively. In the 9 groups, Group $\bar{1}$ is a group of cut holes, Group $\bar{15}$ and Group $\bar{13}$ are groups of perimeter holes, and all holes between the cut and perimeter holes are referred to as auxiliary holes. In order to eliminate the superposition effect of stress wave caused by explosion and reduce the influence of blasting vibration on adjacent structures, the layer-by-layer initiation from inside to outside is realized.

3. Analysis on filed monitoring data

3.1. Monitoring scheme

Three-vector vibration velocity sensor and TC-4850 automatic acquisition system (made in Chengdu Zhongke Instruments Co., Ltd.) are used in the process of blasting vibration monitoring. According to the principle of blasting vibration monitoring and the propagation law of stress wave [11], the monitoring points were located on the side wall of the blasting face in the existing tunnel. As shown in Figure 3, three key monitoring points were arranged in existing tunnel each excavation blasting, which were named as C1, C2, and C3, respectively. And a three-dimensional velocity sensor is installed for each monitoring point to test horizontal radial (PPV_x), horizontal tangential (PPV_y) and vertical vibration velocities (PPV_z). Since the location of each monitoring point is relatively flat and the relative height difference between the monitoring point and others is very small, so the influence of height difference on the propagation of blasting stress wave can be neglected in the analysis of testing data [12,13].

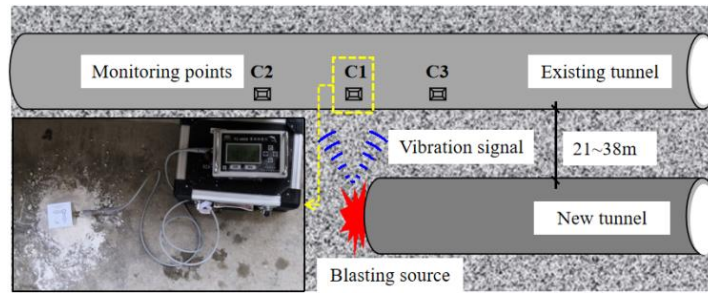


Figure 3. The arrangement blasting vibration monitoring points.

3.2. Analysis of monitoring results

At present, many scholars have proposed the prediction formulas for blasting vibration [14,15], which is basically based on Sadovsky's empirical formula, and the parameters are revised and perfected in actual blasting engineering. Previously, the equation for predicting the relationship between PPV, explosive charge and safe distance are also proposed in China, and has been incorporated into the Blasting Safety Regulations. The PPV can be predicted as follows:

$$PPV = K(Q^{1/3} / R)^\alpha = K[PD]^{-\alpha} \tag{1}$$

$$[PD] = R / Q^{1/3} \tag{2}$$

$$Q_{max} = (PPV / K)^{3/\alpha} R^3 \tag{3}$$

where PPV is the peak particle velocity (cm/s); Q is the maximum charge pre delay (kg); R is the linear distance from the blasting source to monitoring points (m); K, α are the related parameters of blasting vibration, which are related to rock characteristics, site conditions, blasting methods, etc.; $[PD]$ is the proportional distance ($m/kg^{1/3}$).

Four monitoring sections (YK2+558, YK2+550, YK2+546, and YK2+541) were selected in the cross section of new tunnel. And three monitoring points were arranged in existing tunnel during each monitoring section, so a total of 12 sets of data were analyzed by regression analysis. The blasting test results of each monitoring point are shown in Table 2.

Table 1. Tunnel blasting parameters.

Parts	Hole types	Detonator group	Holes depth (m)	Holes number	Charge density (kg/m)	Charge per hole (kg)	Sum charge (kg)	Total charge (kg)
Upper step excavation	Cut holes	1	1.5	12	0.90	1.40	16.80	98.40
	Relief holes	3	1.5	6	0.60	1.00	6.00	
	Auxiliary holes A	5	1.3	4	0.64	0.80	3.20	
	Auxiliary holes B	7	1.3	8	0.64	0.80	6.40	
	Auxiliary holes C	9	1.3	16	0.64	0.80	12.80	
	Inner holes A	11	1.3	22	0.45	0.60	13.20	
	Inner holes B	13	1.3	26	0.45	0.60	15.60	
	Perimeter holes	15	1.3	47	0.15	0.20	9.40	
	Floor holes	17	1.3	15	0.72	1.00	15.00	

Lower step excavation	Floor holes	$\bar{1}$	1.3	7	0.45	0.60	4.20	
	Auxiliary holes A	$\bar{3}$	1.3	14	0.72	1.00	14.00	
	Auxiliary holes B	$\bar{5}$	1.3	19	0.64	0.80	15.20	51.60
	Auxiliary holes C	$\bar{7}$	1.3	21	0.50	0.60	12.60	
	Perimeter holes	$\bar{9}$	1.3	28	0.15	0.20	5.60	

Table 2. Blasting monitoring results.

Monitoring sections	Monitoring points	Maximum charge per delay (kg)	Distance from blasting source (m)	PPV (cm/s)			Main frequency (Hz)		
				PPV _X ^a	PPV _Y ^a	PPV _Z ^a	F _X ^b	F _Y ^b	F _Z ^b
YK2+558	C1		32.4	4.20	0.93	2.30	142.86	129.03	160.00
	C2	16.8	47.5	1.76	0.52	0.86	160.00	19.98	166.67
	C3		43.3	1.87	1.48	1.05	64.52	80.00	121.21
YK2+550	C1		34.4	2.65	1.21	1.19	105.26	51.28	57.14
	C2	16.8	36.8	2.40	0.94	1.33	160.00	61.54	200.00
	C3		54.4	1.34	0.63	0.69	56.92	42.55	102.58
YK2+546	C1		32.5	2.62	1.61	1.33	71.43	19.51	52.63
	C2	15.2	66.4	1.01	0.30	0.37	137.93	48.78	72.73
	C3		61.2	1.08	0.69	0.66	65.57	40.40	51.28
YK2+541	C1		32.0	3.36	1.03	1.38	137.93	38.10	137.93
	C2	16.8	41.9	2.21	0.79	0.98	117.65	55.56	190.48
	C3		38.9	2.29	0.92	1.23	90.91	71.43	142.86

^aPPV_X, PPV_Y, PPV_Z are the maximum particle vibration velocity of horizontal radial, horizontal tangential and vertical, respectively.

^bF_X, F_Y, F_Z are the main frequency of horizontal radial, horizontal tangential and vertical, respectively.

According to the statistical data of PPV in Table 2, the non-linear fitting between the blasting vibration velocity and the corresponding proportional distance in formula (1) and (2) is analyzed, then the corresponding attenuation parameters K and α of stress wave propagation are determined, thus the attenuation curves of PPV in all directions are obtained (Figure 4). The regression empirical formula (4) is as follows:

$$\begin{cases} PPV_X = 206.02 [PD]^{-1.636}, R^2 = 0.9347 \\ PPV_Y = 45.067 [PD]^{-1.414}, R^2 = 0.6049 \\ PPV_Z = 103.38 [PD]^{-1.644}, R^2 = 0.8747 \end{cases} \quad (4)$$

As Figure 4 shows that the PPV of three directions are similar with the change of proportional distance. The peak velocities first show an exponential attenuation law as a whole, then the attenuation rate is faster and finally tends to flat. The main reason is that the pressure produced by the shock wave near the blasting source far exceeds the tensile strength of the rock, which is used to break the rock and consume most of the energy, resulting in a sharp attenuation of the PPV. The attenuation law is basically consistent with Sadovsky's empirical formula, that is, the PPV of each directions decreases

with the increase of the blast center distance.

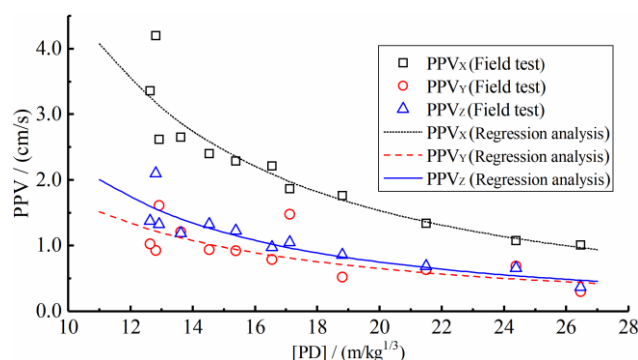


Figure 4. The regression curve of PPV.

It can be found that the maximum PPV is 4.20 cm/s, which is less than the allowable value of 10 cm/s in Blasting Safety Regulations, indicating that the excavation blasting will not damage or affect existing tunnels. The actual statistics of PPV are given in Table 2. Comparing the PPV in each direction, the PPV_x is largest, PPV_z is second, and PPV_y is the smallest, which indicates that the front-side of the blasting source is subjected by the vertical incidence of the blast stress wave, and the PPV_x is dominant.

Meanwhile, the main frequency of blasting vibration is highly discrete, accounting for 33.3% of 0~60Hz, 30.6% of 60~120Hz, and 36.1% of 120Hz~, and generally higher (more than 19.51Hz), but the natural frequency of most underground structures are lower [16,17], so high-frequency vibration is not easy to resonate with the structure, the structure safety mainly depends on the PPV, and the details are shown in Table 2.

4. Numerical Simulation

4.1. Finite element model establishment

To reduce the influence of boundary effect, the left and right boundary of the model are about 3~5 times of the tunnel excavation diameter respectively, so the width of the model is 120 m, the upper boundary is 55 m according to the tunnel depth and the lower boundary is 25 m; The length of the model is 80 m, the blast section is in the middle model, so a 3D finite-element calculation model with a size of 80 m (length) \times 120 m (width) \times 80 m (height) was developed, as shown in Figure 5(a). Due to the charge of the cutting hole is the largest, only the cutting hole is considered when establishing the model, and the diameter of the cutting hole is 0.045 m, the depth is 1.5 m, and the spacing arrangement was the same as the in suit conditions, and then the size of the tunnel structures were completely referenced to the design value as presented in Figure 5(b).

In addition, for the convenience of analysis, the surrounding rock around the tunnel is regarded as the homogeneous, continuous and isotropic rock, without considering the effects of joint fissures, fault fracture zones and blasting damage in surrounding rock. The 3D finite-element model consists of four parts, namely rock mass, explosive, existing tunnel lining and air, and the Solid 164 elements are used for mesh division, which are divided into 190,869 nodes and 181,620 elements in total. Among them, Lagrange algorithm is used for rock and existing lining, and ALE multi-material algorithm is used for explosive and air, which can avoid serious grid distortion caused by explosion and realize dynamic analysis of fluid-solid coupling. In the numerical calculation model, the m-kg-s unit system is adopted, and air medium is filled in both excavated and existing tunnels. Except for the free boundary at the top of the model, the other surfaces are applied for non-reflective boundary.

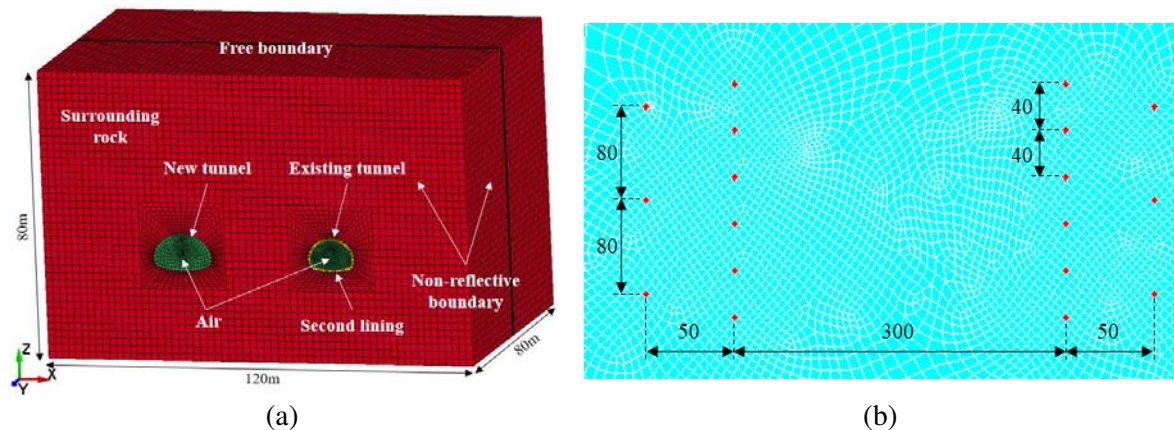


Figure 5. 3D finite element model: (a) 3D model; (b) Cut holes arrangement.

4.2. Model parameters selection

The constitutive relationship between rock mass and existing lining is MAT_PLASTIC_KINEMATIC. This model can not only consider the elastic-plastic properties of rock medium, but also describe the dynamic strengthening, strain rate effect and failure strain of materials [18,19]. Moreover, the constitutive relationship of plastic follower material is based on Cowper-Symonds model, which reflects the relationship between dynamic ultimate yield stress and strain rate factor. The equation (5) is as follows:

$$\sigma_y = \left[1 + \left(\frac{\dot{\varepsilon}}{C} \right)^{1/p} \right] \left(\sigma_0 + \beta \frac{E_0 E_{\tan}}{E_0 - E_{\tan}} \varepsilon_p \right) \quad (5)$$

where σ_y is the dynamic yield stress; $\dot{\varepsilon}$ is the strain rate; ε_p is plastic strain rate; σ_0 is the Initial yield stress; E_0 is Young's modulus; E_{\tan} is the tangent modulus; C , p is the strain rate parameter; β is the hardening parameter; For isotropic hardening, $\beta=1$; And for kinematic, hardening, $\beta=0$. Based on field tests and "Code for Design of Road Tunnel JTG D70-2004" (Chinese National Standard 2004) [20], the physical and mechanical parameters of the rock mass are determined and listed in Table 3.

MAT_NULL material model and EOS_LINEAR_POLYNOMIAL state equation can be used to simulate the constitutive relationship of air in ANSYS/LS-DYNA. The linear polynomial equation of state is linear in internal energy. The pressure is given by:

$$P = C_0 + C_1 \mu + C_2 \mu^2 + C_3 \mu^3 + (C_4 + C_5 \mu + C_6 \mu^2) E_p \quad (6)$$

where P is the blast pressure; E_p is the detonation energy; μ is the specific volume; $C_0 \sim C_6$ is constant of state equation, for ideal gas, when $C_0 = C_1 = C_2 = C_3 = C_6 = 0$, and $C_4 = C_5 = 0.4$ to satisfy the perfect gas equation form; The air density is 1.225 kg/m.

2[#] Rock emulsified explosive is described by MAT_HIGH_EXPLOSIVE_BURN high-energy explosive model and EOS_JWL equation of state, so the formula (7) for calculating explosive pressure is as follows [21]:

$$P(V', E_p) = A \left(1 - \frac{\omega}{R_1 V'} \right) e^{-R_1 V'} + B \left(1 - \frac{\omega}{R_2 V'} \right) e^{-R_2 V'} + \frac{\omega E_p}{V'} \quad (7)$$

where V' is the initial relative volume; A , B , R_1 , R_2 , ω is the explosive material parameters; ρ is the explosive density; D is the detonation velocity. The specific parameters are shown in Table 4.

Table 3. Surrounding rock and existing lining model parameters.

Material	Density (kg/m ³)	E_0 (GPa)	Poisson's ratio	σ_0 (GPa)	E_{tan} (GPa)	β	ε_p
Rock mass	2600	21	0.28	0.175	0.03	0.5	1.25
Existing lining	2350	28	0.17	0.30	0.048	0.5	1.25

Table 4. 2[#] Rock emulsion explosive model parameters.

ρ / (kg/m)	D / (m/s)	P / GPa	A / GPa	B / GPa	R_1	R_2	ω	E_p / (J/m ³)	V'
1120	4300	3.43	42	0.44	3.55	0.16	0.41	3.15	1.00

4.3. Calculation results analysis

4.3.1. Distribution Laws of PPV. To investigate the law of PPV and stress variation of the existing lining structure under explosive load, the element nodes of the existing tunnel lining are extracted. A test section is selected at intervals of 2 m, and 40 groups of test sections are selected, so eight positions are selected on each test section, including the left arch foot, left sidewall, left arch waist, vault, right arch foot, right sidewall, right arch waist and middle invert. All the selected positions represent the key locations of the tunnel structure. Due to limited paper, this paper only lists the time-history curves of the PPV in all directions at the sidewall (No: 95,654) face to blasting source as shown in Figure 6. Specifically, the direction parallel to the tunnel excavation is negative, while the direction of excavation is positive.

In the same test section, the location of the existing lining sidewall is nearest to the blasting source, and the PPV is the largest (Figure 6). The PPV in each direction are 3.79 cm/s (PPV_X), 0.92 cm/s (PPV_Y), 1.90 cm/s (PPV_Z), where: PPV_X > PPV_Z > PPV_Y. The main reason is that the stress wave of the cylindrical charge structure propagates outward in the form of cylindrical waveform at the moment of explosion, and the horizontal radial vibration intensity is the greatest when the stress wave is perpendicularly incident on the tunnel sidewall. Therefore, the PPV_X is dominant, which is agreement with the vibration velocity distribution characteristics in the field test results. It shows that the numerical simulation can better reflect the dynamic response characteristic of the existing lining.

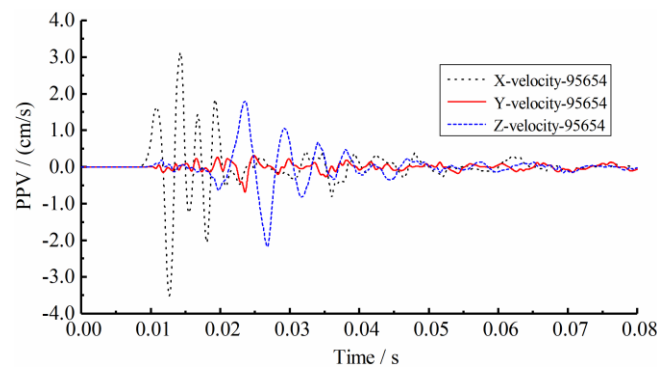
**Figure 6.** Time history curve of PPV in existing tunnel lining sidewall position node.

Figure 7(a) presents the PPV distribution characteristics of existing lining blasting: it can be seen that the PPV at different locations of existing lining is close to the change curve with blasting center distance. On the whole, the PPV is the largest at the same section of blasting excavation face. With the increase of blasting center distance, the PPV decreases gradually. Within the range of 1.5B (about 20m)

from this section, the attenuation rate is faster, and then gradually tends to be flat. Besides, the PPV curve is basically symmetrically distributed with respect to the excavation face. Comparing the PPV of existing lining before and after blasting face, we can see that the attenuation rate of PPV in front of blasting face is slightly lower than that behind. The main reason is that the square behind the blasting excavation is an empty face, and the blast stress wave can not be directly incident on the lining behind the blasting face, but can be reached by diffraction, so some energy is lost, resulting in rapid PPV attenuation.

In addition, it can be seen from Figure 7(b) that the PPV on the front-side of blasting source is obviously larger than that at the backside, and PPV_x is particularly prominent, which indicates that the front-side is greatly affected by the adjacent blasting load, while the backside is less affected and relatively safe because it is mainly affected by the diffraction of blasting stress wave. Therefore, during the blasting excavation, it is necessary to strengthen the monitoring of the PPV on the front-side of blasting source.

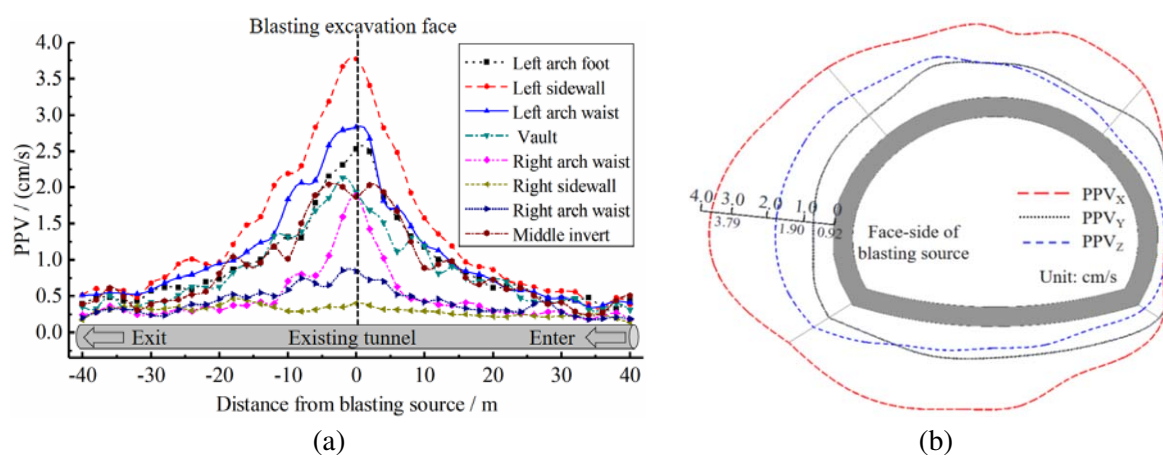


Figure 7. The distribution characteristics of PPV: (a) Longitudinal variation curve; (b) Radial envelope diagram.

4.3.2. Distribution Laws of Stress. Figure 8 shows the longitudinal stress distribution of existing lining. The stress distribution characteristics of existing lining are basically consistent with that the PPV at different locations. Within $1.5B$ of the same section as the blasting face, the tensile stress of existing lining is larger, the maximum value is 0.285 MPa, which is far less than the ultimate tensile strength of lining concrete. Therefore, the adjacent expansion and excavation blasting will not destroy the existing lining. The stress distribution on the front-side of blasting source is as follows: the left sidewall > the left arch waist > the left arch foot > vault. What's more, the PPV is the largest from the sidewall to the arch line of the front-side, and the maximum tensile stress is concentrated in this part, which is mainly affected by the vertical reflection and tension action of the stress wave, so it is easy to produce crack failure.

Figure 9 shows the stress cloud chart of lining at different times. When $t = 10$ ms, the stress peak appears at the left sidewall position, and the maximum value is 0.285 MPa; When $t = 15$ ms, the stress wave appears at the vault position, the maximum value is 0.173 MPa. In this process, the peak stress area gradually transfers to the backside, and the peak stress decreases obviously. Therefore, the peak stress on the backside will be delayed to a certain extent, which indicates the time-history of the stress wave propagation along the radial direction of the lining. With the increase of the distance from blasting source, the existing lining is affected by the oblique incidence of stress wave, and the stress decreases gradually from the blasting source to the outside. The stress distribution on both sides of blasting face is basically symmetrical, while the stress on the front-side of blasting source is the largest,

and the stress response on the backside is not obvious.

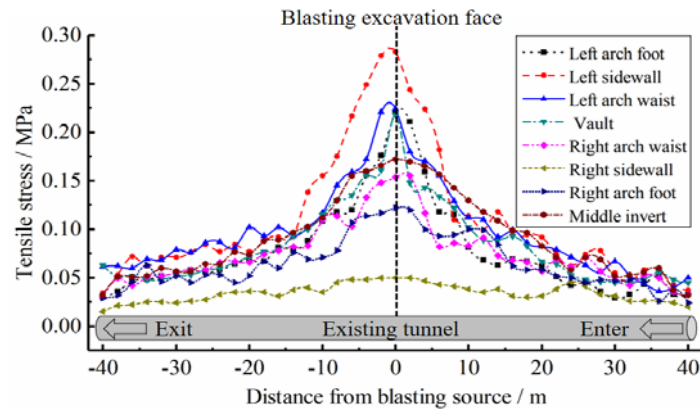


Figure 8. Longitudinal stress distribution of existing lining.

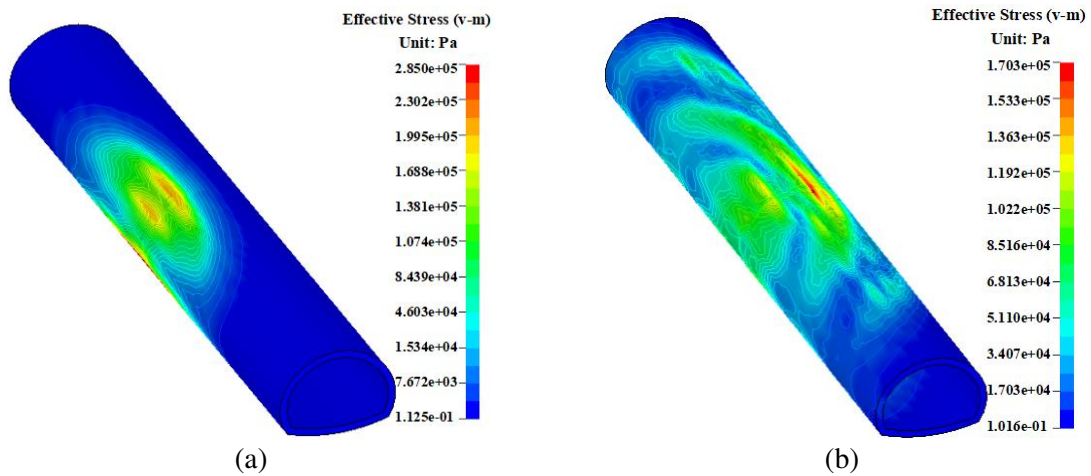


Figure 9. Cloud chart of existing lining stress distribution (unit: Pa): (a) 10 ms; (b) 15 ms.

4.3.3. Comparative Analysis. In order to verify the accuracy of the numerical simulation in expanded tunnel, the maximum PPV_x of each monitoring point in the sidewall position of existing lining (same as the field test position) is extracted, and the field test is compared with the numerical simulation result, as shown in Figure 10. It can be seen that the numerical simulation and field test results show a linear positive correlation, and the relative error is less than 12.1%. Considering the complexity of engineering geology and the idealization of numerical simulation, etc, it is reasonable to have a certain deviation within the allowable range.

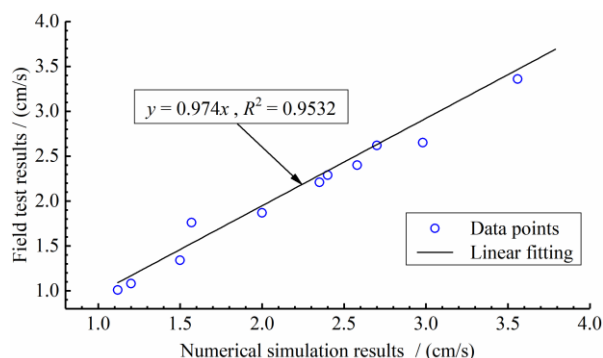


Figure 10. Comparison of field test and numerical simulation results.

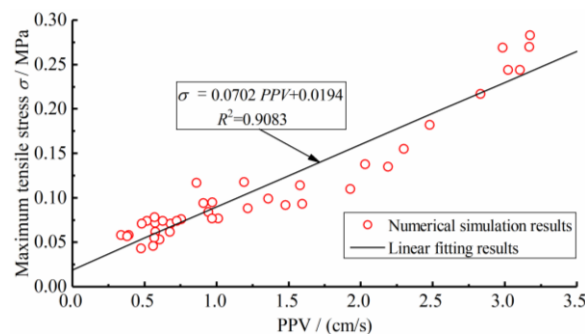


Figure 11. The relationship between maximum tensile stress and PPV of existing lining structure.

5. Discussion on blasting safety control standard

5.1. Safety criterion of PPV

To investigate the influence of PPV and tension stress on the safety of tunnel lining structure, the maximum tension stress and PPV on the sidewall position of existing tunnel lining are statistically analyzed. As shown in Figure 11, the linear fitting relationship between maximum tension stress and PPV is obtained.

$$\sigma = 0.0702PPV + 0.0194, R^2 = 0.9083 \quad (8)$$

where σ is maximum tension stress (MPa), other symbols have the same physical meaning as before.

Eq (8) shows that the fitting correlation coefficient is close to 1, which indicates that there is a linear relationship between the PPV and the peak tensile stress. According to the ultimate tensile stress criterion, when the tensile stress is greater than the ultimate tensile strength of lining concrete, the lining will cause tensile failure. The existing tunnel lining adopts C25 reinforced concrete with a thickness of 55 cm. The dynamic elastic modulus and dynamic tensile strength of concrete structure increase under blasting load. However, considering the unfavorable factors such as service life of existing lining and cumulative blasting damage, the ultimate tensile strength of existing lining is determined to be 1.30 MPa [8,22]. That is, when the PPV exceeds 18.24 cm/s, the peak tensile stress of the existing tunnel lining reaches the ultimate tensile strength, and the lining structure will be damaged. Considering the safety of tunnel lining structure, the revised coefficient of engineering importance is 1.7 [23], and the safety criterion of existing lining PPV is 10.73 cm/s. Besides, because of the high frequency of blasting stress wave, the impact on concrete lining is limited, so it is not necessary to consider the impact of blasting vibration frequency on lining structure.

5.2. Safety control of charge

Generally, under the conditions similar to geological and rock properties, the parameters K and α related to blasting vibration are basically the same. Therefore, $K=206.02$ and $\alpha=1.636$ are selected from the formula (4). When the location of adjacent structures is determined, the maximum charge quantity is mainly determined by the safety PPV. In other words, the relationship curve between the maximum charge quantity and the blasting center distance can be obtained by formula (3) at a certain safe PPV = 10.73 cm/s, as shown in Figure 12.

As can be seen from Figure 12, when the tunnel excavation approaches the existing tunnel gradually, the intensity of blasting vibration should be strictly controlled to reduce the damage of blasting construction to the existing lining structure. When the distance between blasting source and existing lining is nearest 21 m, and the maximum allowable charge should be controlled within 41.05

kg. It can be seen that a single-segment allowable charge in the design of blasting network is within the allowable range, which will not affect the safety of existing tunnel lining structure.

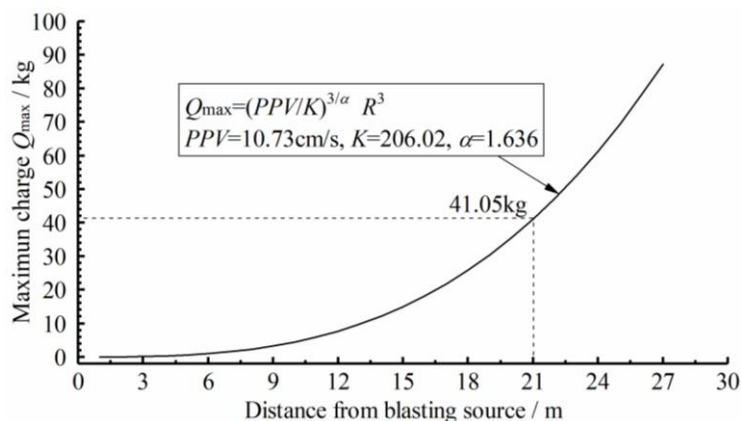


Figure 12. Maximum charge control curve.

6. Conclusions

Based on the expansion project of Erzhuangke Tunnel, this paper aims to investigate the influence of existing tunnel lining under the close blasting load through field test and numerical simulation. The primary conclusions can be summarized as follows: the corresponding attenuation parameters K , α of stress wave are determined by regression analysis of the field monitoring data, and then the regression equations of PPV in different directions are obtained, and the PPV mainly depends on the maximum charge and the distance from blasting source. It is difficult to resonate with the structure when the main frequency is high, so the safety of the structure depends mainly on the PPV. Moreover, the 3D finite element simulation results show that the PPV of the existing lining is the largest at the same section position as the blasting source. With the increase of the distance from the blasting source, the PPV of existing lining decreases gradually, and the both sides are basically symmetrically distributed with the blasting excavation face, while the existing lining within the range of about $1.5B$ from blasting source is greatly affected by the blasting vibration. And the stress distribution is too. The PPV and stress at front-side of tunnel lining are obviously larger than that of backside, so some measures should be taken to focus on protection. The PPV_x is larger than those of other directions, and it dominates. The numerical simulation results have been confirmed by field blasting tests. In addition, the safety control criterion is proposed according to the linear fitting relationship between the PPV and the maximum tensile stress. Combining with the ultimate tensile stress criterion of concrete, the safety PPV of existing lining structure is obtained to be 10.73 cm/s. In order to ensure the safe operation of the existing tunnel under the blasting of the close-distance expansion tunnel, the maximum allowable charge for a single group should be controlled within 41.05kg.

Acknowledgments

This research was financially supported by the Applied Basic Research Project (main subject) of the China Communications Construction Co., Ltd. (No. HT-A-2018-006). And also the author thanks the 5th Branch of CCCC Second Harbor Engineering Co., Ltd. for the support of field test. Finally, the authors are grateful to the reviewers for their precious comments and advice, which were helpful for the improvement of this paper.

References

- [1] Jiang N and Zhou C B 2012 Blasting vibration safety criterion for a tunnel liner structure *Tunn. Undergr. Sp. Tech.* **32** 52-7

- [2] Yu H T, Yuan Y, Yu G X, *et al.* 2014 Evaluation of influence of vibrations generated by blasting construction on an existing tunnel in soft soils *Tunn. Undergr. Sp. Tech.* **43** 59-66
- [3] Shin J H, Moon H G and Chae S E 2011 Effect of blast-induced vibration on existing tunnels in soft rocks *Tunn. Undergr. Sp. Tech.* **26** 51-61
- [4] Yi C P, Lu W B, Zhang J H, *et al.* 2008 Study on critical failure vibration velocity of arch with vertical wall lining subjected to blasting vibration *Rock and Soil Mechanics* **29** 2203-8
- [5] Jiang N, Zhou C B, Luo G, *et al.* 2012 Blasting vibration safety criterion of railway tunnel concrete lining *Journal of Central South University (Science and Technology)* **43** 293-7
- [6] Zhang Q S, Li L P, Li S C, *et al.* 2008 Experimental study of blasting dynamic vibration of closely adjacent tunnels *Rock and Soil Mechanics* **29** 2655-60
- [7] Cheng Y H, Jiang H and Chen W 2017 Blasting vibration control technology and effect analysis of tunnel underneath ramp *Blasting* **34** 63-7
- [8] Ling T H, Zhang S, Zhang L, *et al.* 2018 Blasting vibration characteristics of transition segment of a branch tunnel *Journal of Vibration and Shock* **37** 43-50
- [9] Jia L, Xie Y P and Li S K 2015 Numerical simulation for impact of blasting vibration on nearby tunnel lining safety *Journal of Vibration and Shock* **34** 173-7+211
- [10] Chinese National Standard 2014 *Safety Regulations for Blasting GB 6722-2014* (Beijing, China: Standards Press of China)
- [11] Yang S Q, Zhou J, and LI X J 2005 Observation and analysis of blasting vibration of highway tunnel with small clear distance *Engineering Blasting* **11** 62-5
- [12] Ling T H 2004 *Blasting Vibration Effect and Active Control of Disasters* (Changsha, China: Central South University)
- [13] Ohtsu H, Sakai K and Hasegawa N 2007 Study on the methodology of estimating the rock classification with the seismic exploration in mountain tunnel construction project *J. Soc Mater. Sci. Jpn.* **56** 820-7
- [14] Zhou S R, Zhou J M, Wang H H, *et al.* 2018 Analysis of blasting parameters optimization and blasting vibration effects of subway excavation *Blasting* **35** 85-9
- [15] Lee J S, Ahn S K and Sagong M 2016 Attenuation of blast vibration in tunneling using a pre-cut discontinuity *Tunn. Undergr. Sp. Tech.* **52** 30-7
- [16] Li Y H, Tang C H and Yu Y L 2006 Spectrum Characteristics of blasting vibration and its engineering application *Engineering Blasting* **6** 1-5
- [17] Wang W 2018 Study on parameters optimization and test of smooth blasting in Yujiaya tunnel with in-situ expansion (Xi'an, China: Chang'an University)
- [18] Lu W B, Yang J S, Chen M, *et al.* 2011 An equivalent method for blasting vibration simulation *Simul. Model. Pract. Th.* **19** 2050-62
- [19] Xu H and Wen H M 2016 A computational constitutive model for concrete subjected to dynamic loading *Int. J. Impact Eng.* **91** 116-25
- [20] Chinese National Standard 2004 *Code for Design of Road Tunnel JTG D70-2004* (Beijing: China Communications Press)
- [21] Liu D, Gao W X, Sun B P, *et al.* 2016 Numerical simulation of blasting vibration of existing tunnels *Rock and Soil Mechanics* **37** 3011-6
- [22] Lu S W, Zhou C B, Jiang N, *et al.* 2015 Effect of excavation blasting in an under-cross tunnel on airport runway *Geotech Geol Eng* **33** 973-81
- [23] Chinese National Standard 2014 *Seismic Code for highway engineering JTG B02-2013* (Beijing, China: China Communications Press)